Regulation of force and unloaded sliding speed in single thin filaments: effects of regulatory proteins and calcium

Earl Homsher, David M. Lee, Carl Morris, Dmitry Pavlov and Larry S. Tobacman*

*Department of Physiology, School of Medicine, UCLA, Los Angeles, CA 90095 and *Department of Internal Medicine, University of Iowa, Iowa City, IA 52242, USA*

(Received 6 October 1999; accepted after revision 22 December 1999)

1. Measurements of the unloaded sliding speed of and isometric force exerted on single thin filaments in *in vitro* motility assays were made to evaluate the role of regulatory proteins in the control of unloaded thin filament sliding speed and isometric force production.

2. Regulated actin filaments were reconstituted from rabbit F-actin, native bovine cardiac tropomyosin (nTm), and either native bovine cardiac troponin (nTn), troponin containing a TnC mutant, CBMII, in which the sole regulatory site in cardiac TnC (site II) is inactivated (CBMII-Tn), or troponin containing a point mutation in TnT (I79N, where isoleucine at position 79 is replaced with asparagine) associated with familial hypertrophic cardiomyopathy (FHC).

3. Addition of regulatory proteins to the thin filament increases both the unloaded sliding speed and the isometric force exerted by myosin heads on the thin filaments.

4. Variation of thin filament activation by varying $[Ca^{2+}]$ or the fraction of CBMII/TnC bound to the thin filament at pCa 5, had little effect on the unloaded filament sliding speed until the fraction of the thin filament containing calcium bound to TnC was less than 0·15. These results suggest that $[Ca^{2+}]$ primarily affects the number of attached and cycling crossbridges.

5. The presence of the FHC TnT mutant increased the thin filament sliding speed but reduced the isometric force that heavy meromyosin exerted on regulated thin filaments. These latter results, together with the increased sliding speed and isometric force seen in the presence of regulatory proteins, suggest that thin filament regulatory proteins exert significant allosteric effects on the interaction of crossbridges with the thin filament.

The role of the regulatory proteins (tropomyosin, Tm and troponin, Tn) in the control of muscle contraction is broadly viewed as one of control of the access of the crossbridge to the actin portion of the thin filament. This view epitomized by the 'steric blocking' mechanism of muscle (H. E. Huxley, 1972), is supported by the facts that: (1) regulatory proteins exert little or no effect on the acto-myosin ATPase V_{max} although they elicit a marked rise in K_{ATPase} (Lehrer & Morris, 1982; Williams *et al.* 1988); (2) the positioning of tropomyosin/troponin controls access of the S1 head to strong binding sites on actin, primarily in subdomain 1 and the interface between subdomains 1 and 3 (Xu *et al.* 1999); (3) the isometric force exerted by muscle fibres is proportional to the thick and thin filament overlap (Gordon *et al.* 1966; Edman, 1979) and is a monotonic function of the calcium bound to the thin filaments (Moss, 1992; Wang & Fuchs, 1994); (4) unloaded shortening velocity, V_u, in whole muscle is independent of the number of crossbridges interacting. V_u changes by less than 10% over sarcomere lengths from 1·7 to 3·1 μm during tetanic stimulation while isometric force is proportional to thick and thin filament overlap (Gordon *et al.* 1966; Edman, 1979). This view is consistent with A. F. Huxley's (1957) crossbridge model (1) which predicts that the unloaded shortening velocity in muscle is independent of the number of crossbridges attached to the thin filament but is limited by a drag imposed on thin filament sliding by strongly bound crossbridges.

Despite this evidence, a number of observations suggest that the regulatory proteins can themselves alter the interaction between the S1 head and the actin filament in ways that may modulate specific steps in the acto-S1ATPase reaction mechanism. These observations include: (1) tropomyosin bound to actin inhibits ATPase activity at low stoichiometric ratios of S1:actin and stimulates it at intermediate ratios of S1:actin (Lehrer & Morris, 1982; Williams *et al.* 1988); (2) strongly bound crossbridges (e.g. NEM S1) at sub-saturating $[Ca^{2+}]$ increase the rate of acto-S1 ATPase of regulated thin filaments and potentiate

isometric force production and the rate of rise of force in skinned muscle fibres (Williams *et al.* 1988; Swartz & Moss, 1992); (3) variation of myofibrillar [Ca^{2+}] alters not only isometric force and rate of force redevelopment (k_{tr}), but also unloaded shortening velocity in skinned single muscle fibres (Julian, 1971; Brenner, 1988); (4) familial hypertrophic cardiomyopathy (FHC) is expressed in persons whose cardiac myocytes contain a mutant TnT or Tm and it has been suggested that these changes in the regulatory proteins may alter the myocardium's ability to produce force and shorten in a normal fashion (Sweeney *et al.* 1998; Tobacman *et al.* 1999). Further, replacement of regulatory proteins (TnT or Tm) by mutant regulatory proteins associated with FHC produces changes in thin filament sliding speed in motility assays and in acto-S1 ATPase rates (Lin *et al.* 1996; Bing *et al.* 1997*a*,*b*; Tobacman *et al.* 1999). These observations raise the possibility that regulatory proteins exert allosteric effects as well as controlling access of the crossbridge to the thin filament.

To evaluate the mechanical effects of regulatory proteins on the interaction between crossbridges and thin filaments, we measured the thin filament unloaded sliding speed, V_f, and force, P_f, exerted on single reconstituted thin filaments attached to calibrated micro-needles in *in vitro* motility assays. This approach affords the experimenter complete control of the proteins constituting a contractile unit and thus permits performance of structure–function studies using various proteins which were not possible with intact muscle. The thin filaments examined were those containing: rabbit F-actin alone; rabbit F-actin, bovine ventricular tropomyosin (nTm) and troponin (nTn) at various Ca^{2+} concentrations; rabbit F-actin, nTm, and variable ratios of nTn and a troponin chimera (CBMII-Tn) containing a mutant troponin C (CBMII-TnC) which cannot bind calcium and thus cannot be activated (Putkey *et al.* 1989; Huynh *et al.* 1996); and F-actin, nTm and a troponin chimera (mutTn) containing a mutant TnT (I79N, where isoleucine at position 79 was replaced with asparagine) expressed in certain patients having FHC (Lin *et al.* 1996; Sweeney *et al.* 1998). These measurements revealed that the addition of regulatory proteins to F-actin increases both V_f and P_f, but although regulated thin filaments containing I79N TnT increased thin filament sliding speed, it reduced isometric force. These results show that the regulatory proteins control more than just the access of S1 to actin and supports the notion that regulatory proteins exert allosteric effects on the interaction of S1 and actin. Measurement of the isometric force–pCa curve in regulated thin filaments produced data similar to those seen in single skinned muscle fibres while the sliding speed–pCa curve was displaced almost 1 pCa unit from the pK (−log of the dissociation constant) for the force–pCa curve. Variation of the thin filament activation by incorporation of variable amounts of CBMII-Tn into the thin filaments at saturating [Ca^{2+}] varied the relationship between the extent of thin filament activation and V_f in a fashion comparable to that seen by varying the [Ca^{2+}] in thin filaments reconstituted from F-actin, nTn and nTm. This result implies that the effect of [Ca^{2+}] in the regulation of unloaded shortening speed is to control the number of crossbridges interacting with the thin filament as opposed to changing the rate or the size of the power stroke.

METHODS

Protein preparation

Rabbits were handled and killed (120 mg kg^{-1} pentobarbitone I.V.) according to protocols approved by the Chancellor's Animal Research Committee at UCLA. Rabbit skeletal myosin was prepared from white back and leg muscles as described by Margossian & Lowey (1982). The myosin was stored in 50% (v/v) glycerol at −20 °C and used within 6 weeks of preparation. Rabbit skeletal heavy meromyosin (HMM) was prepared as described by Kron *et al.* (1991) and stored on ice for up to 5 days. Actin was purified from rabbit muscle acetone powder as described by Pardee & Spudich (1982), and used for up to 2 months after preparation. Bovine ventricular tropomyosin (Tm) and troponin (Tn) were purified as described by Tobacman & Adelstein (1986). Troponin chimeras containing a wild-type cardiac TnT or the I79 cardiac TnT mutation were prepared as described by Lin *et al.* (1996) while those containing the CBMII mutation were prepared as described by Huynh *et al.* (1996). The Tm and Tn proteins were stored for up to 12 months at −80 °C in 10 mM Tris (pH 7·5), 1 mM dithiothreitol (DTT), 0·01% NaN_3, 5 μg ml^{-1} each of L-1-tosylamide 2-phenylethyl chloromethyl ketone (TPCK) and *N*-α-p-tosyl-L-lysine chloromethyl ketone (TLCK), and 0·3 mM phenylmethylsulfonyl fluoride (PMSF).

Reconstitution and rhodamine–phalloidin labelling of thin filaments

Rhodamine–phalloidin (RP) labelled F-actin was prepared as described previously (Homsher *et al.* 1996) and used within 2 weeks. Reconstitution of regulated thin filaments from actin, Tm and Tn was achieved by mixing the proteins at a concentration of 0·67 μM F-actin, 0·17 μM Tm and 0·16 μM Tn in actin buffer. The solution was incubated overnight before use.

Microneedle fabrication and calibration

Microneedles were pulled from borosilicate glass rods (1 mm o.d.) to an initial tip diameter of 10–20 μm and then a final diameter of ca. 0·5 μm (Howard & Hudspeth, 1988). The ultra-compliant glass whisker was cut to a final length of 300–600 μm before use. The microneedle stiffness was calibrated as described by VanBuren *et al.* (1994). At least five calibrations were performed on each needle with a variation of $\leqslant$ 10% about the mean for each. The stiffness of the microneedles used ranged from 1 to 15 pN μm^{-1}.

Force measurements

Nitrocellulose-coated coverslips and flow cells were prepared as previously described (Homsher *et al.* 1996) with minor modifications. We used glass coverslips (24 mm × 60 mm, No. 0) to create an incubation chamber over which a coverslip (18 mm × 18 mm, No. 1) was placed to provide an optically flat surface. For the attachment of HMM, the lower coverslip was coated with ~1 μl of 0·2% nitrocellulose in amyl acetate. To allow manipulation of the microneedle, 1 mm thick glass spacers separated the top and bottom surfaces of the flow cell. An HMM solution (300 μg ml^{-1}) was injected into the chamber and replaced 2 min later by 350 μl of 0·5 mg ml^{-1} bovine serum albumin in assay buffer (25 mM Mops, 25 mM KCl, 2 mM $MgCl_2$, 1 mM DTT, pH 7·4). One minute later 450 μl activating solution was introduced into the flow cell. The

activating solution contained 25 mM Mops (pH 7·4), 26·1 mM KCl, 2 mM $MgCl_2$, 2 mM EGTA (with varying ratios of CaKEGTA or K_2EGTA), 1 mM Na_2-ATP, 100 nM Tm and Tn (of the form used in the experiments), and 40 mM DTT. The solution also contained 14 mM glucose, 240 units of glucose oxidase ml^{-1} (Sigma, St Louis, MO, USA), and 9×10^3 units of catalase ml^{-1} (Sigma) to slow photo-bleaching (Kron *et al.* 1991). The ionic strength (50 mM) and pCa of the activating solution were calculated as previously described (Lin *et al.* 1996).

The flow cell was placed on the stage of a Leica DMIRB inverted microscope. Under epifluorescence illumination (100 W Hg-arc lamp, ×100 PL Fluotar objective lens, NA = 1·3) 0·5 μl of 1·5 nM RP labelled thin filaments (an actin 'cloud') was injected into the activating solution. The fluorescent filaments were imaged on a VE 1000 SIT camera (DAGE-MTI, Michigan City, IN, USA) and recorded without enhancement on a Sony VCR. The microneedle was held at an angle of 4–5 deg to the HMM coated surface and moved by a joystick controlled MP-285 three-dimensional micromanipulator (Sutter Instrument Co., Novato, CA, USA). The needle tip had been coated with a layer of nitrocellulose (0·2% in amyl acetate). It was next coated with α-actinin (2 mg ml^{-1}; Cytoskeleton, Denver, CO, USA) by placing the tip in a 10 μl droplet on the coverslip just outside the flow cell for 10 min. Under ×100 bright field illumination, the α-actinin coated needle was rinsed with assay buffer and manoeuvred into the motility chamber to a position near the actin 'cloud'. A thin filament, 10–20 μm in length, was brought into contact with the microneedle and allowed to bind to the needle tip. The microneedle was then lowered to 2–3 μm above the motility surface to allow the attached thin filament to diffuse to and interact with the HMM on the surface. As the filament was pulled by the HMM, the microneedle tip was deflected. The microneedle was re-positioned so the filament was pulled perpendicular to the microneedle axis. The maximal maintained displacement of the needle tip and the length of thin filament in contact with the surface were measured from videotaped sequences using an Argus 10 image processor (Hamamatsu, Middlesex, NJ, USA). Measurements for a given filament (i.e. the maximum deflection and the length of actin in contact with the motility surface) were repeated at least 3 times and the mean calculated. The force exerted on the filament was computed from the product of the average maintained displacement and the microneedle stiffness. The force exerted by each thin filament was regressed against the length of thin filament in contact with the surface using least-squares regression analysis (SigmaPlot 4.0, SPSS, Inc., Chicago, IL, USA). The regression yielded a slope (significantly different from zero) expressing the force exerted per micrometre length of thin filament. The standard error of the regression slope (S.E.R.) averaged 0·04 of the slope. The correlation coefficient, r^2, for these plots ranged from 0·79–0·99 and none of the y-intercepts were significantly different from zero. Unless otherwise noted, all experiments were performed at 22–23 °C and an ionic strength of 50 mM. The microscope and manipulators were mounted on a pneumatic-vibration isolation table.

Estimation of the number of myosin heads on the motility surface

The number of myosin molecules bound to the motility surface was estimated using the technique of Uyeda *et al.* (1990). Our measurements indicated that HMM bound to the motility surface according to a binding isotherm whose apparent K_m was 168 ± 45 μg HMM ml^{-1} and was saturated at 3850 ± 30 HMM μm^{-2} of motility surface. From these measurements we estimate that in our experiments there are 4935 ± 430 myosin heads μm^{-2}. Assuming that a myosin head can bind to a 6 nm diameter actin filament within 10 nm of either side of it, then as many as 130 ± 11 myosin heads on the motility surface are available to bind to each micrometre length of thin filament.

Motility measurements

Quantification of the thin filament sliding speed was performed using a motion analysis system (Santa Rosa, CA, USA). The speed data were obtained from the same slides as the force measurements. The data were acquired and analysed as previously described (Homsher *et al.* 1996) and are expressed as means ± S.E.M.

RESULTS

Force and sliding speed of unregulated thin filaments over the motility surface

The force exerted on unregulated filaments and the sliding speeds of these filaments was measured first. Measurements were made at pCa 5 and pCa 9. Because the measurements at the two pCa values were no different, observations from both were pooled. Figure 1 shows the force exerted by thin filaments of various lengths bound to the HMM coated surface. As reported earlier for unregulated filaments (VanBuren *et al.* 1994), force was a linear function of the length of thin filament bound to the surface. The slope of the linear regression of force exerted *vs.* thin filament length bound to the motility surface is an estimate of the isometric force exerted per unit length of F-actin in contact with the surface. Regression analysis indicates that the HMM on the surface exerted a force of 8·25 ± 0·46 pN μm^{-1} actin bound to the surface (mean ± S.E.M., $n = 8$ observations). Table 1 contains the average thin filament sliding speed observed in the same preparations in which isometric force was measured. It averaged 3·33 ± 0·03 $\mu m\ s^{-1}$.

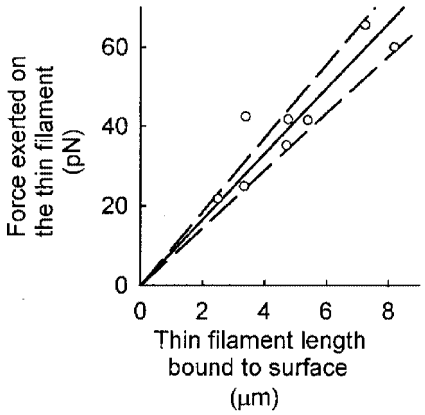

Figure 1. Force *versus* thin filament length of unregulated thin filaments on motility surface

The relationship between the maximum force and the length of thin filament in contact with the HMM surface for unregulated thin filaments moving over HMM-coated surfaces at pCa 9 and 5. Each data point represents an individual thin filament measurement. The least-squares linear regression fits to the data (continuous lines) and the 95% confidence limits (dashed lines) were constrained through the origin. Data for this plot are summarized in Table 1.

Table 1. Effect of regulatory proteins on thin filament mechanics

Conditions	Force (pN μm^{-1})	Sliding speed ($\mu m\ s^{-1}$)
Unregulated	8·25 ± 0·46 (8)	3·33 ± 0·03 (432)
nTn (pCa 5)	12·36 ± 0·40 (15)	4·60 ± 0·03 (345)
nTn (pCa 6)	8·48 ± 0·20 (12)	4·29 ± 0·04 (228)
nTn (pCa 6·5)	2·88 ± 0·21 (10)	3·65 ± 0·03 (351)
nTn (pCa 7·5)	0·96 ± 0·10 (7)	1·41 ± 0·01 (16)
nTn (pCa 8 or 9)	0 (9)	0·03 ± 0·02 (205)
wtTnT (pCa 5)	12·63 ± 0·80 (8)	4·86 ± 0·06 (306)
mutTnT (pCa 5)	9·35 ± 0·35 (15)	5·20 ± 0·06 (174)
nTnT (pCa 5) $I/2 = 100$ mM	—	4·43 ± 0·04 (431)
mutTnt (pCa 5) $I/2 = 100$ mM	—	5·51 ± 0·03 (401)

Force and sliding speed measurements were taken from the same flow cell chamber. Data are given as means ± S.E.R. (force) or S.E.M. (sliding speed). Numbers in parentheses are the number of filaments observed. Unregulated, F-actin containing no regulatory proteins; nTn, thin filaments composed of F-actin, native Tm and native cardiac Tn; wtTnT, thin filaments composed of F-actin, native Tn and Tn containing wild-type TnT; mutTnT, thin filaments composed of F-actin, native Tm and Tn containing the Ile79Asn TnT mutant. Ionic strength, $I/2$, 50 mM except where otherwise noted.

The effect of regulatory proteins on maximal force and unloaded thin filament sliding speed. The force exerted by regulated thin filaments and their unloaded sliding speed was measured at pCa values ranging from 5 to 9. Figure 2*A* and *B* shows plots of the steady state force generated by skeletal HMM at pCa 5, 6, 6·5 and 7·5 against the length of regulated thin filament in contact with the motility surface. Similar measurements were made at pCa 8 and 9 but no significant force or shortening velocities were observed. The slopes of these plots (P_f) (along with the unloaded thin filament sliding speed, V_f) are given in Table 1. A striking aspect of these measurements is that the addition of regulatory proteins to the thin filaments produced an increase in both P_f and V_f at pCa 5 compared to F-actin thin filaments. The maximal isometric force exerted on regulated thin filaments at pCa 5 is almost 50% greater ($P < 0·01$, Student's unpaired t test) than that exerted by unregulated thin filaments (Table 1). The thin filament sliding speed of regulated thin filaments increased by 38% ($P < 0·001$).

To determine if one or both of the regulatory proteins altered the thin filament sliding speed, F-actin filaments bound to the HMM-coated motility surface were incubated in a motility solution (lacking ATP) in the absence of regulatory proteins, with only Tm (500 nM), only Tn (500 nM), or with Tm and Tn (500 nM each). To measure V_f at pCa 5, the incubation solutions were replaced, respectively, by a motility solution containing no regulatory proteins, 100 nM Tm, 100 nM Tn or 100 nM Tm and Tn. The effects of these different treatments are shown in Fig. 3. They show that Tm has no significant effect on V_f, but addition of Tn alone or in the presence of Tm promotes a marked increase in V_f. These data indicate that the change in V_f is directly related to the effects of Tn in the presence of saturating calcium concentrations.

Dependence of isometric force and sliding speed on $[Ca^{2+}]$ in regulated thin filaments

A second important result obtained from the measurements in Fig. 2 is shown in Fig. 4 (○) and Table 1. Here the slopes of the linear regressions of force against the length of the thin filament bound to the surface at pCa 5, 6, 6·5, 7·5 and 8 for regulated thin filaments decrease progressively and are

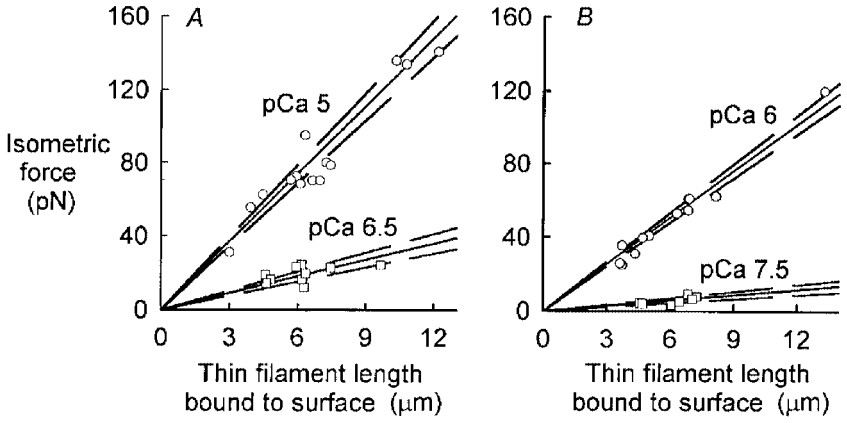

Figure 2. Maximal isometric force and length of regulated thin filament in contact with the motility surface at various pCa values

A, data taken at pCa 5 (○) and 6·5 (□). *B*, data taken at pCa 6 (○) and 7·5 (□). The continuous lines are least-squares regressions through zero and the dashed lines to either side are the 95% confidence lines. Data for this plot is summarized in Table 1.

significantly different from each other ($P < 0{\cdot}001$, Student's t test). These isometric force data are plotted in Fig. 4 and are well fitted ($r^2 > 0{\cdot}99$) by a Hill equation of the form $P/P_o = 1/(1 + 10^{n_H(pCa - pK)})$ where pK is $6{\cdot}19 \pm 0{\cdot}33$ (mean ± S.D.) and n_H, the Hill coefficient, is $1{\cdot}66 \pm 0{\cdot}12$ (mean ± S.D.).

The thin filament unloaded sliding speed measured in the same experiments as the isometric force was dependent on $[Ca^{2+}]$ as shown in Table 1 and Fig. 4 (open squares). Fits of the normalized data to the Hill equation (Fig. 5) show that the relationship between filament sliding speed and pCa has a pK of $7{\cdot}1 \pm 0{\cdot}12$ (mean ± S.D.) and a Hill coefficient of $1{\cdot}1 \pm 0{\cdot}23$ (mean ± S.D., and $r^2 > 0{\cdot}99$). At pCa 8, less than 1% of the thin filaments bound to the HMM coated surface exhibited any movement. None of the filaments moved at pCa 9. Figure 5 shows that the pK for the V_f–pCa relationship is shifted strongly to the left of the force–pCa curve. The large difference in pK for the two curves implies that the factors limiting the speed and isometric force are different.

At pCa 8 and 9 thin filaments bind to the surface, probably via weak electrostatic binding (Miller & Reisler, 1995), but do not slide over the surface when they are unloaded and produce no measurable deflection (less than 0·125 μm) of the microneedle tip under isometric conditions. No deflection of the microneedle tip (< 0·5 μm) was detected even when the microneedle was slowly moved (at an average speed of 3·7 μm s^{-1}) to drag the attached thin filaments (average length $14{\cdot}3 \pm 1{\cdot}9$ μm, mean ± S.E.M., $n = 5$) over the surface. If a 0·5 μm microneedle displacement did occur and was undetected, the drag force on the thin filaments would be less than $0{\cdot}38 \pm 0{\cdot}07$ pN μm^{-1} (mean ± S.E.M., $n = 5$), or less than 1·8% of the maximum isometric force. These observations suggest that the drag between the thin filament and the motility surface is negligible.

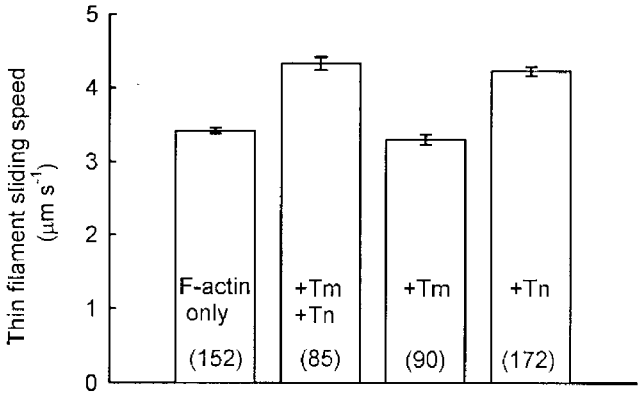

Figure 3. The effect of regulatory proteins on thin filament sliding speed

Bar graph of the unloaded thin filament sliding speeds obtained from unregulated thin filaments (F-actin only), thin filaments incubated for 8 min on motility surface in the presence of 500 nM nTm/nTn (+Tm +Tn), 500 nM nTm (+Tm), or 500 nM nTn (+Tn). In the motility measurements the solution bathing the surface was at pCa 5 and contained 100 nM Tm and Tn (+Tm +Tn), 100 nM Tm (+Tm), or 100 nM Tn (+Tn). The columns and error bars are means ± S.E.M. The number of thin filaments used to compute the mean is given in parentheses.

Effect of variations of thin filament activation on thin filament sliding speed at saturating $[Ca^{2+}]$

If $[Ca^{2+}]$ controls the number of crossbridges interacting with the thin filament, the unloaded sliding speed will be independent of $[Ca^{2+}]$ until too few crossbridges are attached to produce continuous movement of the thin filament. Alternatively, if $[Ca^{2+}]$ varies the rate or extent of the crossbridge throw then varying the number of crossbridges at saturating $[Ca^{2+}]$ (pCa 5) will have no effect on thin filament sliding speed. To evaluate this hypothesis, the effect of thin filament activation at pCa 5 on V_f was measured. Thin filaments were reconstituted at pCa 5 using varying ratios of native Tn (nTn) and Tn containing CBMII (CBMII-Tn) (Huynh *et al.* 1996). Because CBMII-Tn cannot bind calcium, thin filament sites at which CBMII-Tn binds are inhibited. The fraction of the thin filament binding sites occupied by nTn (fractional thin filament Ca^{2+} binding) was calculated at a given ratio of nTn/(nTn + CBMII-Tn) using empirical binding constants (Huyhn *et al.* 1996) for pCa 5. Thin filament sliding speed was then measured at these different ratios at pCa 5. Figure 5 shows that thin filament sliding speed was essentially constant as the fractional thin filament Ca^{2+} binding was reduced and fell by only 11%

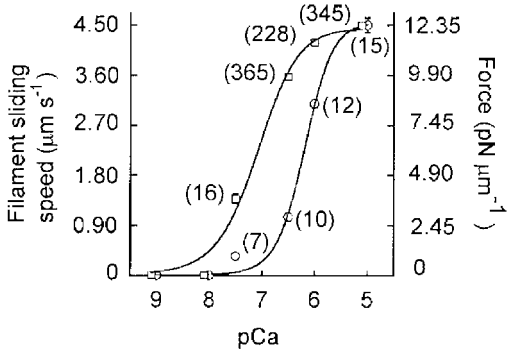

Figure 4. Force–pCa and speed–pCa curves

Calcium dependence of unloaded sliding speed (□) and steady-state isometric force (○) for regulated thin filaments at 50 mM ionic strength. Each data point gives the mean and S.E.M. for the measurement. The number of filaments from which observations were made is given in parentheses near each point. At pCa 8 and 9 no filaments were sliding, and the number of filaments from which isometric force measurements were attempted at pCa 8 and 9 was 6 and 3, respectively. The data are plotted so that the maximal speed and force are the same distance above 0 so that the relative sliding speed and force can be gauged on an absolute scale. The lines are least-squares regression fits to the individual data points. The fitting parameters for the sliding speed are $n = 1{\cdot}1 \pm 0{\cdot}2$ and p$K = 7{\cdot}1 \pm 0{\cdot}1$ and for the force are $n = 1{\cdot}7 \pm 0{\cdot}1$ and p$K = 6{\cdot}2 \pm 0{\cdot}3$ (mean ± S.E.R.).

from its maximal value when the fraction of Tn binding sites occupied by CBMII-Tn was 88%. Further reduction in nTn/(nTn + CBMII-Tn) causes V_f to fall toward zero. When the thin filament sliding speed data obtained at various pCa are plotted in Fig. 6 (using the fractional isometric force as a measure of the thin filament activation at various pCa values) the results are similar to those obtained by varying the nTn/(nTn + CBMII-Tn) at pCa 5. The similarity of these data to those at different pCa values implies that unloaded filament sliding speed is largely independent of the extent of calcium saturation of troponin and is directly related to the number of crossbridge heads pulling on the thin filament.

Effect of the I79N TnT mutation on force production in regulated thin filaments

We have previously shown that thin filaments reconstituted with nTn containing the I79N TnT mutant exhibit the same actomyosin ATPase and Ca^{2+} affinity as those reconstituted from native TnT (Lin *et al.* 1996). However, in the *in vitro* motility assay, reconstituted thin filaments containing this TnT mutant (mutTn) exhibited an increased unloaded sliding speed (ca. 40%) compared with thin filaments containing the native (nTnT) or wild-type TnT (wtTnT). This change was not associated with a shift in the Ca^{2+} sensitivity of filament sliding speed. Sweeney *et al.* (1998) have shown that skinned cardiac myocytes transfected by and expressing the I79N mutant TnT exhibit an elevated unloaded shortening velocity and produce less force than those expressing wild-type TnT. They suggested that the hypertrophy seen in the presence of this mutation is a compensatory adaptation to the altered force–velocity relationship. Microneedle force measurements were used here to determine if the maximum force exerted on regulated thin filaments by the HMM surface was similarly affected by the mutTn. Table 1 shows the isometric force exerted by the HMM on thin filaments containing nTn, wtTn, or mutTn at pCa 5 was 12·36 ± 0·4, 12·64 ± 0·79, and 9·38 ± 0·35 pN μm^{-1} (means ± S.E.R.), respectively. The presence of the mutTn reduced the isometric force exerted on regulated thin filaments by 25% ($P < 0{\cdot}0001$, Student's t test). The maximum isometric forces exerted on thin filaments containing either the nTn (12·36 pN μm^{-1}) or wtTn (12·64 pN μm^{-1}) were not significantly different from each other ($P > 0{\cdot}1$, Student's t test). In the same experiments, the sliding speeds for thin filaments containing nTn, wtTn or mutTn were 4·60 ± 0·03, 4·86 ± 0·06 and 5·20 ± 0·06 $\mu m\ s^{-1}$ (means ± S.E.M., $n = 174$–306 filaments), respectively. The presence of the mutTn produced a significant 11% increase ($P < 0{\cdot}001$, Student's t test) in sliding speed compared with that in nTn at 50 mM ionic strength. This result differs quantitatively from our earlier report, i.e. the presence of the mutTn resulted in 40% faster sliding speed at 100 mM ionic strength (Lin *et al.* 1996). To learn whether differences in ionic strength might contribute to this discrepancy, thin filament sliding speed was measured at 100 mM ionic strength (Table 1). In this case, the presence of the mutTn (5·51 ± 0·03, mean ± S.E.M., $n = 431$) produced 24% faster sliding speeds ($P < 0{\cdot}001$, Student's t test) than the nTn controls (4·43 ± 0·03, mean ± S.E.M., $n = 401$).

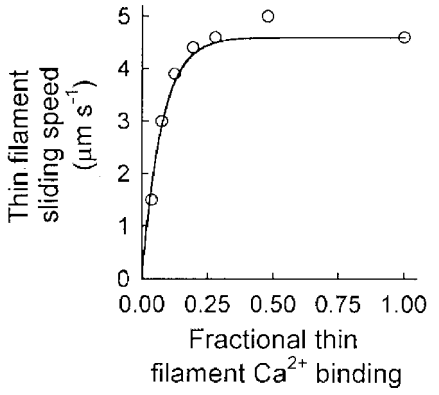

Figure 5. The effect of fractional calcium binding to the thin filaments on thin filament sliding speed

Data are given as means ± S.E.M. The continuous line is a best-fit hyperbolic relationship to all the data.

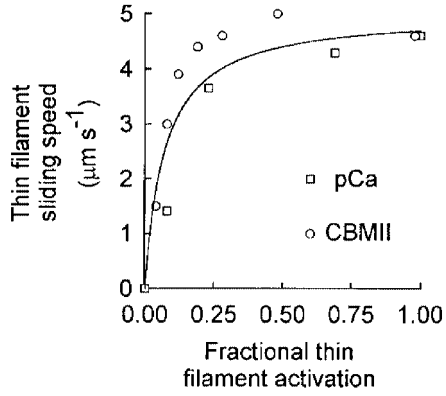

Figure 6. Comparison of different methods of activation on thin filament sliding speed

Data from Fig. 5 (○) is superimposed on data from Table 1 and Fig. 2 from experiments in which the pCa was varied (□). In the latter case the fractional thin filament activation was taken as the microneedle force relative to that at saturating calcium, pCa 5. The continuous line is a non-linear least-squares fit to the equation of Ueyda *et al.* (1990) describing the thin filament sliding speed in terms of the size of the crossbridge throw (d), the duty cycle duration (t_s), at unloaded sliding speed, the maximal ATPase rate (k_{cat}) at 25 °C (25 s^{-1}). N is the number of attached crossbridges at any point in time, so that:

$$\text{sliding speed} = d/t_s \times (1 - (1 - t_s \times k_{cat})^N).$$

In this formulation d/t_s is the maximal sliding speed, 4·6 $\mu m\ s^{-1}$. At full activation 130 crossbridges can interact with the thin filament per micrometre yielding a sliding speed of 4·6 $\mu m\ s^{-1}$. Taking d as 10 nm (Homsher *et al.* 1996), t_s must be 2·17 ms. $N = 130x$, where x is the fractional thin filament activation.

DISCUSSION

The effects of regulatory proteins on crossbridge–actin interaction

The increased isometric force and unloaded thin filament sliding speed observed in the presence of regulatory proteins were unexpected. The maximal rate of ATP hydrolysis by actin and myosin S1 heads, V_{max}, is unaffected by the presence or absence of regulatory proteins at pCa 5 at roughly equivalent molar equivalents of actin and myosin heads (Williams *et al.* 1988). However, when the myosin head concentration is reduced to less than 0·2 of the actin concentration in the presence of regulatory proteins, V_{max} falls to ~20% of its maximal value, despite the fact that the F-actin concentration necessary to reach 50% of the maximal ATPase (K_{ATP}) rate is unchanged (Williams *et al.* 1988). Measurements of actomyosin ATPase rates in solution are made at low ionic strength (13 mM) and the interaction of the myosin heads with the actin filament are mechanically unconstrained. In motility assays and muscle fibres, interaction between the myosin heads and thin filament are subjected to marked mechanical constraints which demonstrably affect the rate of ATP hydrolysis (Siemankowski *et al.* 1985; Woledge *et al.* 1985; Ma & Taylor, 1994). Although the unloaded shortening velocity is roughly proportional to the actomyosin (AM) ATPase rate over four orders of magnitude (Barany, 1967), the ATPase rate is not limited by the rate of crossbridge detachment from the thin filament (Ma & Taylor, 1994). At physiological [ADP] and [ATP], the rate of ADP release from the AM.ADP complex, which does limit the unloaded thin filament sliding speed, is 10–100 times faster than the actomyosin ATPase V_{max} (Siemankowski *et al.* 1985).

Might the binding of the regulatory proteins to the thin filament stiffen it and cause the crossbridge to more efficiently and rapidly push the thin filament in the motility assay? If this were the case the persistence length (L_p, a measure of the thin filament stiffness) of actin should be markedly increased by the presence of regulatory proteins. However, the persistence length of F-actin is 9 μm and increases to just 12 μm in the presence of regulatory proteins and calcium (Isambert *et al.* 1995). Further, Tm addition to the thin filament increases L_p to 21 μm, but the thin filament sliding speed is not significantly changed (Fig. 3). These results suggest that a change in thin filament stiffness cannot account for the increased sliding speed and force observed in the presence of regulatory proteins.

Which regulatory proteins produce the changes in force and unloaded thin filament sliding speed? The experiments shown in Fig. 3 show that the presence of Tn produces a significant increase in V_f, but Tm does not. These results agree with those of Bing *et al.* (1997*a*), who found that Tm or Tm + TnI + TnC binding to the thin filament does not increase thin filament sliding speed beyond that of actin alone. However, when skeletal Tm and skeletal Tn, skeletal Tm + skeletal TnI + TnC + TnT, or cardiac Tm and cardiac Tn are bound to the thin filament, the regulated thin filament sliding speed is increased over that of actin alone by ~30%. These results suggest that TnT acts in concert with TnI and TnC to increase V_f. The extended amino terminus of TnT binds to both the overlapping regions of adjacent tropomyosin molecules and to actin. TnT interaction with TnC, TnI and Tm both increases inhibition of actomyosin ATPase in the absence of Ca^{2+} and increases stimulation in the presence of Ca^{2+} (Potter *et al.* 1995). These results are consistent with the increased thin filament sliding speed seen upon replacement of native TnT with the I79N FHC TnT (Lin *et al.* 1996; Tobacman *et al.* 1999). Finally, other regulatory protein mutations have been linked to an increased thin filament sliding speed in motility assays. These include FHC TnT mutations ΔExon-15,16 and E244D (Tobacman *et al.* 1999), and FHC Tm mutations D175R and Q180G (Bing *et al.* 1997*b*). These mutant regulatory proteins increase regulated thin filament unloaded sliding speed by 6–21% over thin filaments containing native or wild-type regulatory proteins. Studies in which cultured cardiac myotubes were transfected with and expressed I79N or R92Q TnT produced a 2-fold increase in unloaded shortening velocity and the I79N reduced the maximal isometric force to 75% of its control value (Sweeney *et al.* 1998). This behaviour of the I79N TnT containing myotubes is consistent with the observations made in the force and sliding speed reported here.

Insight as to how regulatory proteins affect the crossbridge cycle may be gained by considering the steps in the crossbridge cycle.

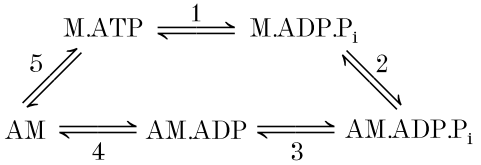

Scheme 1

Scheme 1 represents a minimalist series of reaction steps for the crossbridge ATPase mechanism. Strain-dependent values for each of the rate constants for the steps have been modelled in a way which accounts for the observed force–velocity curve, isometric force, unloaded shortening velocity, and their dependence on ATP, ADP and P_i (Pate & Cooke, 1989). In this model M.ADP and M.ADP.P_i are detached crossbridge states, AM.ADP.P_i is a weakly attached crossbridge, and AM.ADP and AM are strongly attached force exerting states. It is also very likely that steps 3, 4 and 5 are composed of two steps each (an isomerization and a dissociation step). Because regulatory proteins are unlikely to affect the behaviour of detached states, only steps 2–5 should be affected by the addition of regulatory thin filament proteins. Examination of the Pate & Cooke (1989) model reveals that: (1) increases in the forward (clockwise)

rate constants of steps 2 and 3 significantly increase isometric force, P_{max}, but have little effect on unloaded shortening velocity, V_u; and (2) increases in the forward rate constants of steps 3, 4, or 5 increase V_u but only 4 and 5 have a slight negative or no effect on P_{max} (for a summary of the effects of changes in these rate constants see Table 8, Regnier *et al.* 1998). Increasing the forward rate of step 5 markedly increases the unloaded shortening velocity but has no effect on isometric force or ATPase rate. It may be that the binding of regulatory proteins to the thin filament changes the myosin interaction surface of actin so that the a combination of changes in the rate constants of steps 2–5 occur to produce an increased force and unloaded sliding speed. Alternatively, once bound to the thin filament, the crossbridge head might itself interact with the regulatory proteins, thereby altering the rate constants of one or more of steps 2–5. Because the rates of these steps are strain dependent (there is not simply one fixed rate), it is possible that changes occur primarily at negative or positive strains. Nevertheless, changing the interaction between the thin filament and its substrate (M.ADP.P_i) by effects at a separate site interacting with the regulatory proteins is, by definition, an allosteric effect.

Relation to studies in single muscle fibres

The microneedle force–pCa curve (Figs 4 and 5) (n_H, 1·7; pK, 6·2) is comparable to those of skinned cardiac cells (Hofmann *et al.* 1991) and skinned skeletal fibres whose endogenous TnC was replaced with cardiac TnC (Moss, 1992). Thus the single regulated thin filament behaves very similarly to skinned muscle fibres. These results suggest that at reduced [Ca^{2+}], either fewer crossbridges are attached and pulling on the thin filament or the force exerted per crossbridge is reduced. The constancy of the force/stiffness ratio as pCa is reduced in skinned muscle fibres (Brenner, 1988) argues for the former interpretation. In motility assays, however, the Hill coefficient is 15–35% less than that for fibres. Two factors may contribute to the reduced co-operativity of the force–pCa curve for *in vitro* motility assays. First, the random array of S1 heads on the coverslip and their less productive attachment to the filaments may reduce the co-operative effects of strongly bound crossbridges (VanBuren *et al.* 1994). Second, the force measurements were made at 50 mM ionic strength, compared with the more physiological value of 200 mM used in fibre experiments. Reductions in n_H are observed at lower ionic strength in both skeletal and cardiac muscle (Fink *et al.* 1986).

The effects of pCa on fibre unloaded shortening velocity are different from its effects on thin filament sliding speed. In fibres, Moss (1986) found that at submaximal pCa unloaded shortening occurred in two phases. An initial fast phase of shortening, whose velocity, V_u, exhibited little dependence on calcium (occurring for shortening of less than 8–10% the muscle length), was followed by a second phase of shortening whose velocity declined in proportion to the reduction in [Ca^{2+}] (Moss, 1986). In the intact muscle fibre whose maximal activation has been reduced by treatment with the E–C coupling inhibitor, dantrolene, no significant change in V_u was observed (Edman, 1979). This discrepancy may stem from the fact that in Edman's (1979) experiments, the distance shortened at reduced pCa was always less than 10% of the muscle length. Further dantrolene treatment may produce a non-uniform reduction in pCa throughout the fibre diameter, i.e. it may inhibit calcium release deep in the fibre but not at the fibre surface. The effects of pCa observed on sliding speed in the motility assays more closely resembles the effects of calcium on the initial phase of the unloaded shortening velocity. The lack of correspondence between the motility sliding speed and the second phase of unloaded shortening in skinned muscle fibres suggests that the second phase is related to constraints present in the skinned fibre but absent in the isolated thin filament.

Unlike the V_f–pCa data reported here and elsewhere (Homsher *et al.* 1996; Gordon *et al.* 1997), Fraser & Marston (1995) reported only a 30% reduction in V_f at very low calcium concentrations using silanized motility surfaces. When they used nitrocellulose-coated surfaces (as in the current study) they found a marked drop in V_f (Bing *et al.* 1997*a*). They attributed the different behaviour between the two surfaces to the presence of a drag present on nitrocellulose-treated surfaces which is absent on silanized motility surfaces. Unlike Bing *et al.* (1997*a*), we observed no filament sliding at pCa 8 or 9 (Fig. 4) over either nitrocellulose-coated or silanized surfaces (E. Homsher & N. Back, unpublished results). Our interpretation of the significant sliding speeds Fraser & Marston (1995) observed at pCa 8 and 9 is that the [Tn] in their motility assay was too low to completely regulate the thin filament. The thin filament sliding seen at pCa 8 and 9 was due to thin filaments with Tm but no Tn bound. This interpretation is supported by similarity of the V_f at pCa 8 and 9 to that of unregulated thin filaments.

The role of calcium in regulating force and sliding speed

Two hypotheses have been proposed to explain the [Ca^{2+}] regulation of muscle contraction. The first was a 'recruitment' model derived from the steric blocking model of contraction (H. E. Huxley, 1972). In this model calcium binding to TnC is an 'on/off' switch, which controls the number of crossbridges bound to the thin filament but does not alter the rate of crossbridge attachment to or detachment from the thin filament or the rate or extent of the power stroke (Podolsky & Teichholz, 1970). The second hypothesis is a 'kinetic' model, in which calcium binding to TnC modulates the rate of crossbridge attachment to or detachment from the thin filament or the rate or extent of the power stroke (Julian, 1971; Brenner, 1988). The recruitment model as originally proposed cannot be correct because crossbridges bind (albeit weakly) to thin filaments in the absence of calcium (Brenner *et al.* 1982). Further the increase in steady state ATPase rate as [Ca^{2+}] rises is far out of proportion to the change in crossbridge binding to actin

(Chalovich *et al.* 1981). The rate of force redevelopment (k_{tr}) in fibres varies with pCa (Brenner, 1988; Millar & Homsher, 1990; Walker *et al.* 1992) while the simplest recruitment model predicts that k_{tr} will be independent of the pCa. The kinetic model of regulation originally suggested that calcium regulated the rate of P_i release from the actomyosin crossbridge (Chalovich & Eisenberg, 1982) which corresponds to a regulation of the power stroke. The apparent independence of the rate of P_i release in isometrically contracting muscles at various pCa (Millar & Homsher, 1990; Walker *et al.* 1992) implies, however, that calcium regulation occurs at a step prior to P_i release, but after weak binding to the thin filament. This result implies, according to Scheme 1, that calcium regulates a crossbridge step after step 2 but before step 3, i.e. a transition from a weakly bound crossbridge to a strongly bound crossbridge that has not produced any force. The data in Figs 4–6 support this view, because thin filament sliding speed (which is most affected by changes in steps 3, 4 and 5) fell by less than 20% when reductions in [Ca^{2+}] reduced the isometric force by greater than 75% (which are strongly affected by changes in the rates of steps prior to 3, 4 and 5). The similarity of alterations in sliding speed due to changes in pCa and changes in number of available actin binding sites at pCa 5 (in CBMII-Tn) (Fig. 6) indicates that the change in speed is less related to the pCa than to the number of attached crossbridges.

The behaviour of unloaded thin filament sliding speed is similar to that reported earlier in that reduction of [Ca^{2+}] slows regulated thin filament sliding speed (Fraser & Marston, 1995; Homsher *et al.* 1996; Gordon *et al.* 1997). At first glance this result seems contradictory to A. F. Huxley's (1957) postulate that unloaded shortening velocity is limited by the rate of crossbridge detachment from the thin filament. However, as Uyeda *et al.* (1990) have shown, this is true only if there are large numbers of crossbridges (>75) interacting with a filament. In motility assays thin filament length ranges from 1–15 μm and given the crossbridge density this means that 130–1950 crossbridges can interact with the thin filament. However, if the number of accessible actin sites is reduced to 10% of maximal, the number of crossbridges pulling on the thin filament must fall to 13–195 for the thin filaments. Given a duty cycle of 2·17 ms and a maximal turnover rate of 25 s^{-1}, this would yield sliding speeds of 0·52–1·0 of maximal (see legend to Fig. 6 for details of calculation). In the fibre thin filaments are arranged in parallel and 1000 thin filaments (Woledge *et al.* 1985) are attached to each side of the Z line per myofibril. Thus if only one crossbridge could attach per thin filament, there would be 1000 crossbridges pulling on each side of the Z line in a myofibril.

In both isometric and isotonic conditions the power stroke rapidly follows strong binding, succeeded by product release, ATP binding, and S1–ATP dissociation from actin. The rate at which weakly bound crossbridges enter into the strongly bound force-generating state will be calcium dependent, if there is a Ca^{2+}-dependent equilibrium step (weak to strongly bound but non-force exerting crossbridge attachment) prior to the power stroke itself. This mechanism would then account for the well-documented effect of [Ca^{2+}] on the rate of rise of force (Brenner, 1988). Because a Ca^{2+}-regulated transition from a weakly to strongly bound non-force generating state would not contribute to thin filament motion, unloaded thin filament sliding speed would be independent of the extent of thin filament activation as long as there are enough crossbridges attached to constantly and uniformly propel the thin filament. When insufficient numbers of actin molecules are exposed to assure constant movement of the thin filament, sliding speed will fall (Uyeda *et al.* 1990).

Relation to FHC mutant regulatory proteins

Isometric force is reduced and unloaded thin filament sliding speed is increased by the presence of the I79N TnT mutant, which agrees well with corresponding measurements in quail myotubes expressing this mutant (Sweeney *et al.* 1998). The TnT mutation in this report and several of those studied by Sweeney *et al.* (1998) are located in a region of troponin forming an extended tail stretching along and binding to the tropomyosin strand (Tobacman, 1996). The similar effects occasioned by the presence of the I79N and R92Q TnT mutations (reduced isometric force and increased V_u) together with the fact that large changes in Tm affinity for actin occur in the presence of S1, Tn and Ca^{2+} suggest these mutations change the actin–Tm interacting surface. Alterations in the actin interaction surface may allosterically produce changes in acto-S1 binding and crossbridge kinetics. If the changes in acto-S1 interaction increase the rate of crossbridge dissociation from actin (R_{51} in the model of Pate & Cooke, 1989), isometric force will be reduced and V_u will rise. The mechanical changes would stem from an altered position of Tm over the actin–Tm interface mediated by alterations in the TnT tail flexibility. The reduced isometric force and increased V_u may then initiate the compensatory hypertrophy seen in familial hypertrophic cardiomyopathy.

Barany, M. (1967). ATPase activity of myosin correlated with speed of muscle shortening. *Journal of General Physiology* **50**, 197–218.

Bing, W., Fraser, I. D. C. & Marston, S. B. (1997*a*). Troponin I and troponin T interact with troponin C to produce different Ca^{2+}-dependent effects on actin-tropomyosin filament motility. *Biochemical Journal* **327**, 335–340.

Bing, W., Rewood, C. S., Purcell, I. F., Esposito, G., Watkins, H. & Marston, S. B. (1997*b*). Effects of two hypertrophic cardiomyopathy mutations in alpha-tropomyosin, Asp175Asn and Glu180Gly, on Ca^{2+} regulation of thin filament motility. *Biochemical and Biophysical Research Communications* **236**, 760–764.

Brenner, B. (1988). Effect of Ca^{2+} on cross-bridge turnover kinetics in skinned single rabbit psoas fibers: Implications for regulation of muscle contraction. *Proceedings of the National Academy of Sciences of the USA* **85**, 3265–3269.

Brenner, B., Schoenberg, M., Chalovich, J. M., Greene, L. E. & Eisenberg, E. (1982). Evidence for crossbridge attachment in relaxed muscle at low ionic strength. *Proceedings of the National Academy of Sciences of the USA* **79**, 88–91.

Chalovich, J. M., Chock, B. & Eisenberg, E. (1981). Mechanism of action of troponin-tropomyosin: inhibition of actomyosin ATPase without inhibition of myosin binding to actin. *Journal of Biological Chemistry* **256**, 575–578.

Chalovich, J. M. & Eisenberg, E. (1982). Mechanism of action of troponin-tropomyosin: Inhibition of actomyosin ATPase activity without blocking the binding of myosin to actin. *Journal of Biological Chemistry* **257**, 2432–2437.

Edman, K. A. P. (1979). The velocity of unloaded shortening and its relation to sarcomere length and isometric force in vertebrate muscle fibres. *Journal of Physiology* **291**, 143–159.

Fink, R. H., Stephenson, D. G. & Williams, D. A. (1986). Potassium and ionic strength effects on the isometric force of skinned twitch muscle fibres of the rat and toad. *Journal of Physiology* **370**, 317–337.

Fraser, I. D. C. & Marston, S. B. (1995). *In vitro* motility analysis of actin-tropomyosin regulation by troponin and calcium. *Journal of Biological Chemistry* **270**, 7836–7841.

Gordon, A. M., Huxley, A. F. & Julian, F. J. (1966). Tension development in highly stretched vertebrate muscle fibres. *Journal of Physiology* **184**, 143–169.

Gordon, A. M., Lamadrid, M. A., Chen, Y., Luo, Z. & Chase, P. B. (1997). Calcium regulation of skeletal muscle thin filament motility *in vitro*. *Biophysical Journal* **72**, 1295–1307.

Hofmann, P. A., Hartzell, H. C. & Moss, R. L. (1991). Alterations in Ca^{2+} sensitive tension due to partial extraction of C-protein from rat skinned cardiac myocytes and rabbit skeletal muscle fibers. *Journal of General Physiology* **97**, 1141–1163.

Homsher, E., Kim, B., Bobkova, E. & Tobacman, L. S. (1996). Calcium regulation of thin filament movement in an *in vitro* motility assay. *Biophysical Journal* **70**, 1881–1892.

Howard, J. & Hudspeth, A. J. (1988). Compliance of the hair bundle associated with gating of mechanoelectrical transduction channels in the bullfrog's saccular hair cell. *Neuron* **1**, 189–199.

Huxley, A. F. (1957). Muscle structure and theories of contraction. *Progress in Biophysical Chemistry* **7**, 255–318.

Huxley, H. E. (1972). Structural changes in the actin- and myosin-containing filaments during contraction. *Cold Spring Harbor Symposium on Quantitative Biology* **37**, 361–376.

Huynh, Q., Butters, C. A., Leiden, J. M. & Tobacman, L. S. (1996). Effects of cardiac thin filament Ca^{2+}: Statistical mechanical analysis of a troponin C site II mutant. *Biophysical Journal* **70**, 1447–1455.

Isambert, H., Venier, P., Maggs, A. C., Fattoum, A., Kassab, R., Pantaloni, D. & Carlier, M. F. (1995). Flexibility of actin filaments derived from thermal fluctuations. Effect of bound nucleotide, phalloidin, and muscle regulatory proteins. *Journal of Biological Chemistry* **270**, 11437–11444.

Julian, F. J. (1971). The effect of calcium on the force-velocity relation of briefly glycerinated frog muscle fibres. *Journal of Physiology* **218**, 117–145.

Kron, S. J., Toyoshima, Y. Y., Uyeda, T. Q. P. & Spudich, J. A. (1991). Assays for actin sliding movement over myosin-coated surfaces. *Methods in Enzymology* **196**, 399–416.

Lehrer, S. & Morris, E. P. (1982). Dual effects of tropomyosin and troponin-tropomyosin on actomyosin subfragment 1 ATPase. *Journal of Biological Chemistry* **257**, 8073–8080.

Lin, D., Bobkova, A., Homsher, E. & Tobacman, L. S. (1996). Altered cardiac troponin T *in vitro* function in the presence of a mutation implicated in familial hypertrophic cardiomyopathy. *Journal of Clinical Investigation* **97**, 2842–2848.

Ma, Y. & Taylor, E. W. (1994). Kinetic mechanism of myofibril ATPase. *Biophysical Journal* **66**, 1542–1553.

Margossian, S. S. & Lowey, S. (1982). Preparation of myosin and its subfragments from rabbit skeletal muscle. *Methods in Enzymology* **85**, 55–71.

Millar, N. C. & Homsher, E. (1990). The effect of phosphate and calcium on force generation in glycerinated rabbit skeletal muscle fibers. *Journal of Biological Chemistry* **265**, 20234–20240.

Miller, C. J. & Reisler, E. (1995). Role of charged amino acid pairs in subdomain-1 of actin in interactions with myosin. *Biochemistry* **34**, 2694–2700.

Moss, R. L. (1986). Effects on shortening velocity of rabbit skeletal muscle due to variations in the level of thin filament activation. *Journal of Physiology* **377**, 487–505.

Moss, R. L. (1992). Ca^{2+} regulation of mechanical properties of striated muscle: mechanistic studies using extraction and replacement of regulatory proteins. *Circulation Research* **70**, 865–884.

Pardee, J. D. & Spudich, J. A. (1982). Purification of muscle actin. *Methods in Cell Biology* **24**, 271–289.

Pate, E. & Cooke, R. (1989). A model of crossbridge action: the effects of ATP, ADP, and Pi. *Journal of Muscle Research and Cell Motility* **10**, 181–196.

Podolsky, R. J. & Teichholz, L. E. (1970). The relation between calcium and contraction kinetics in skinned muscle fibres. *Journal of Physiology* **211**, 19–35.

Potter, J. D., Sheng, Z., Pan, B. & Zhao, J. (1995). A direct regulatory role for troponin T and a dual role for troponin C in the Ca^{2+} regulation of muscle contraction. *Journal of Biological Chemistry* **270**, 2557–2562.

Putkey, J. A., Sweeney, H. L. & Campbell, S. T. (1989). Site-directed mutation of the trigger calcium-binding sites in cardiac troponin C. *Journal of Biological Chemistry* **264**, 12370–12378.

Regnier, M., Lee, D. M. & Homsher, E. (1998). ATP analogs and muscle contraction: mechanics and kinetics of nucleoside triphosphate binding and hydrolysis. *Biophysical Journal* **74**, 3044–3058.

Siemankowski, R. F., Wiseman, M. O. & White, H. D. (1985). ADP dissociation from actomyosin subfragment 1 is sufficiently slow to limit the unloaded shortening velocity in vertebrate muscles. *Proceedings of the National Academy of Sciences of the USA* **82**, 658–662.

Swartz, D. R. & Moss, R. L. (1992). Influence of a strong-binding myosin analogue on calcium-sensitive mechanical properties of skinned skeletal muscle fibers. *Journal of Biological Chemistry* **267**, 20497–20506.

Sweeney, H. L., Feng, H. S., Yang, Z. & Watkins, H. (1998). Functional analyses of troponin T mutations that cause hypertrophic cardiomyopathy: insights into disease pathogenesis and troponin function. *Proceedings of the National Academy of Sciences of the USA* **95**, 14406–14410.

Tobacman, L. S. & Adelstein, R. S. (1986). Mechanism of regulation of cardiac actin-myosin subfragment 1 by troponin-tropomyosin. *Biochemistry* **25**, 798–802.

Tobacman, L. S., Lin, D., Butters, C., Landis, C., Back, N. & Homsher, E. (1999). Functional consequences of troponin T mutations found in hypertrophic cardiomyopathy. *Journal of Biological Chemistry* **274**, 28363–28370.

Uyeda, T. Q. P., Kron, S. J. & Spudich, J. A. (1990). Myosin step size: estimation from slow sliding movement of actin over low densities of heavy meromyosin. *Journal of Molecular Biology* **214**, 699–710.

Vanburen, P., Guilford, W. H., Kennedy, G., Wu, J. & Warshaw, D. M. (1994). Enhanced force generation by smooth muscle myosin *in vitro*. *Proceedings of the National Academy of Sciences of the USA* **91**, 202–205.

Walker, J. W., Lu, Z. & Moss, R. L. (1992). Effects of Ca^{2+} on the kinetics of phosphate release in skeletal muscle. *Journal of Biological Chemistry* **276**, 2459–2466.

Wang, Y. P. & Fuchs, F. (1994). Length, force, and Ca(2+)-troponin C affinity in cardiac and slow skeletal muscle. *American Journal of Physiology* **266**, C1077–1082.

Williams, D. L., Greene, L. E. & Eisenberg, E. (1988). Cooperative turning on of myosin subfragment 1 adenosinetriphosphatase activity by the troponin-tropomyosin-actin complex. *Biochemistry* **27**, 6987–6993.

Woledge, R. C., Curtin, N. A. & Homsher, E. (1985). *Energetic Aspects of Muscle Contraction*, pp. 1–329. Academic Press, San Diego.

Xu, C., Craig, R., Tobacman, L., Horowicz, K. & Lehman, W. (1999). Tropomyosin positions in regulated thin filaments revealed by cryoelectron microscopy. *Biophysical Journal* **77**, 985–992.

Acknowledgements

The authors are indebted to Mahta Nili and C. Butters for their excellent technical support, Dr A. M. Gordon for useful discussion and criticism of the manuscript, and Dr Joe Howard for instruction in the fabrication and use of microneedles. This work was supported by National Institutes of Health grants HL-38834 (L.T.) and AR-30988 (E.H.) and AHA Grant-in-Aid 9650128 N (L.T.).

Corresponding author

E. Homsher: Department of Physiology, School of Medicine, UCLA, Los Angeles, CA 90095, USA.

Email: ehomsher@physiology.medsch.ucla.edu